International Journal of Fracture Mechanics, 2, 1966, pp. 426-447.

# CONTAINED PLASTIC DEFORMATION NEAR CRACKS AND NOTCHES UNDER LONGITUDINAL SHEAR

James R. Rice*

ABSTRACT

An exact linear elastic-perfectly plastic solution is presented for the problem of a sharp notch (or, when the notch angle is zero, a crack) in a plane of finite width subjected to anti-plane stresses inducing a stress and deformation state of longitudinal shear. General solutions for physical coordinates corresponding to given stresses, position of the elastic-plastic boundary, and accompanying displacements are given in terms of finite single integrals.

The case of cracks is treated in detail and closed form solutions are presented in terms of elementary and elliptic functions. Numerical results are given and applications of the solution to the development of fracture mechanics failure criteria, as well as some inherent difficulties, are discussed.

## INTRODUCTION

The exact determination of the influence of plastic yielding on the stress and deformation near the root of a crack or notch is of basic importance for the mechanics of fracture and fatigue. In the absence of relevant exact solutions for tensile loadings acting perpendicular to a crack line and inducing a state of plane strain or generalized plane stress, two distinct approaches have been taken. First, there is the work of Dugdale[1] as extended by Goodier and Field[2] and Rice[3] wherein plastic yielding is handled in an approximate manner (most appropriate for plane stress conditions) by placing constraining yield level tensile stresses along a slit ahead of the crack tip in a manner which ensures bounded and continuous stresses at the edge of the plastic zone. An alternate approach is consideration of the simpler elastic-plastic problems arising under longitudinal shear loadings as in the work of Hult and McClintock[4], McClintock[5], and Koskinen[6]. Here one attempts to reason by analogy with the technically important cases of tensile loadings; McClintock and Irwin[7] have pointed out that several important observed features of yielding around cracks under tensile loadings are preserved in the longitudinal shear case.

The problem solved here of an edge notch, with depth a and angle $2\alpha$ in a plane of width b and of infinite height, subjected to longitudinal shearing stress $\tau$ is shown in Figure 1. Koskinen has treated the same problem in [6] but solved it only for special cases through the approximate numerical scheme of finite differences. The importance of the corresponding tensile problem for practical cases of cracks and notches in finite structures and for fracture toughness and fatigue crack growth test specimens has led the author to consider an exact analytic solution as presented here. The solution for the single edge notched plane of Figure 1 is identical to that in corresponding regions for the doubly edge notched, internally notched, and rigid shearing punch configurations of Figure 2 since symmetry requires that $\tau_{xz}$ vanish on the centerlines for the latter three cases (this equivalence is only approximately true for tensile loadings as indicated by the elastic solutions of [8-11]).

The anti-plane deformation of longitudinal shear involves displacements $w = w(x,y)$ in a direction perpendicular to the $(x,y)$ plane only, and all stresses except the shears $\tau_{xz}$, $\tau_{yz}$ are everywhere zero. Stress equilibrium and isotropic elastic stress-strain relations lead to the conclusion that $\tau_{xz} - i\tau_{yz} = G\left(\frac{\partial w}{\partial x} - i\frac{\partial w}{\partial y}\right)$ is an analytic function of the complex variable $x + iy$ in the elastic region, where G is the shear modulus. Assuming a Tresca (or Mises) yield equation $\sqrt{\tau_{xz}^2 + \tau_{yz}^2} = k$ = yield stress

* Assistant Professor of Engineering, Brown University, Providence, R.I.

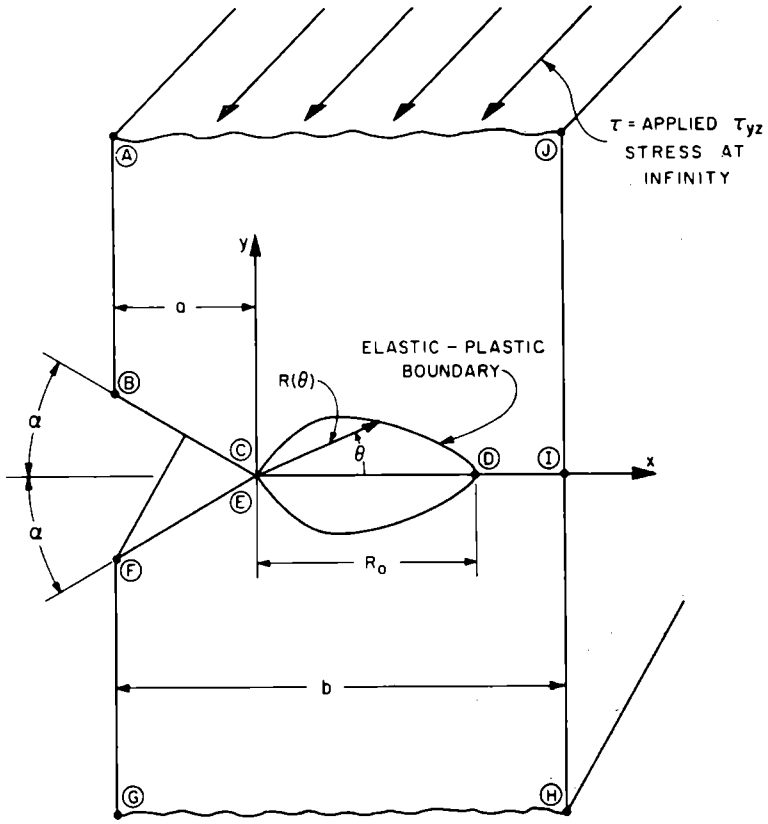


Fig. 1. Problem considered and notation

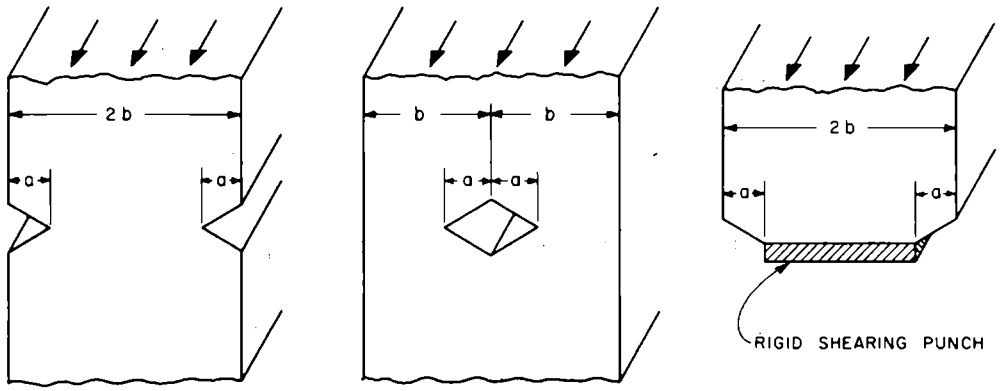


Fig. 2. Equivalent problems

in shear and a Mises type plastic flow rule, Hult and McClintock[4] have shown following the treatment of Prager and Hodge,[12] that in the plastic region stresses and strains are given by

$$\tau_{\theta z} = k, \quad \tau_{rz} = 0 \tag{1}$$

$$\gamma_{\theta z} = \frac{1}{r}\frac{\partial w}{\partial \theta} = \frac{k}{G}\frac{R(\theta)}{r}, \quad \gamma_{rz} = \frac{\partial w}{\partial r} = 0 \tag{2}$$

where $R(\theta)$ is the distance from crack tip to the elastic-plastic boundary as in Figure 1.

## TRANSFORMATION TO STRESS PLANE

Since $\tau_{xz} - i\tau_{yz}$ is an analytic function of $x + iy$ in the elastic region, one has conversely $x - iy$ an analytic function of $\tau_{xz} + i\tau_{yz}$. Making the quantities dimensionless through division by notch depth a and yield stress k,

$$\frac{x - iy}{a} = f'(\zeta) \tag{3}$$

where

$$\zeta = \xi + i\eta = -i\,\frac{\tau_{xz} + i\tau_{yz}}{k} \tag{4}$$

and $f(\zeta)$ is an analytic function for all values of $\zeta$ corresponding to stresses in the elastic domain (that is, for $|\zeta| < 1$). As in [4, 6], through consideration of the direction of the stress vector on the traction free boundary, uniform conditions at infinity, and noting that $|\zeta| = 1$ on the elastic-plastic boundary, the elastic region in the $(x, y)$ plane maps into the slit sector of a unit circle in the $\zeta$ plane as in Figure 3, where points A, B, ..., J correspond to those of Figure 1.

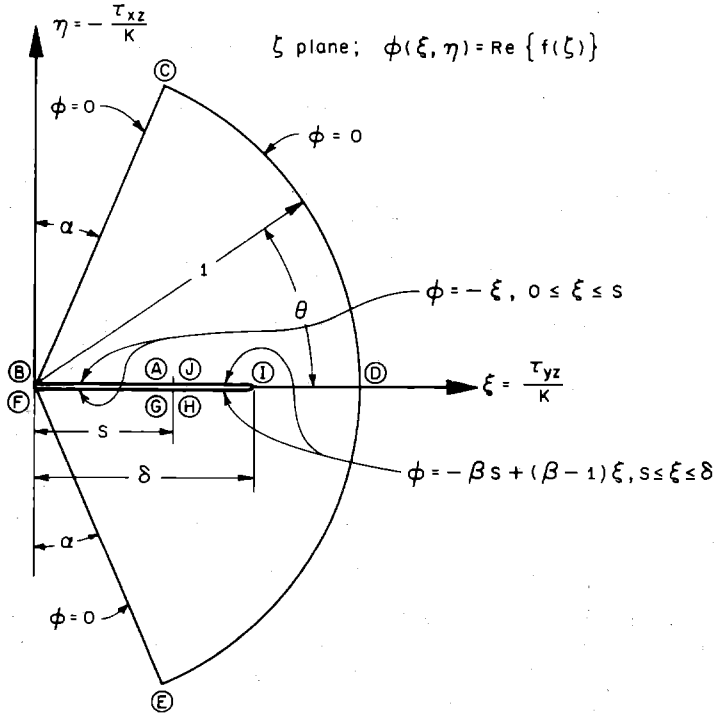


Fig. 3. Map of elastic region in the stress plane

The notations

$$s = \frac{1}{k}\,\tau_{yz}\,\Big|_{y\,=\,\pm\infty} = \frac{1}{k}\,\tau, \tag{5}$$

a dimensionless applied stress, and

$$\delta = \frac{1}{k}\,\tau_{yz}\,\Big|_{x\,=\,b-a,\;\;y\,=\,0} = \frac{1}{k}\,\tau_I \tag{6}$$

are introduced where the dimensionless stress $\delta$ at point I is to be determined from the condition that $f'(\delta)$ be bounded, since $x - iy$ is a continuous function of $\tau_{xz} + i\tau_{yz}$ in the neighborhood of point I. From the stress solution in the plastic zone of (1), the angle $\theta$ of Figure 3 is identical to the angle $\theta$ of Figure 1 for corresponding points on the elastic-plastic boundary.

Boundary conditions are given in terms of a harmonic function $\phi(\xi,\eta)$ where

$$\phi(\xi,\eta) = \mathrm{Re}\,\{f(\zeta)\} \tag{7}$$

and, from (3) with Cauchy-Riemann equations,

$$\frac{\partial\phi}{\partial\xi} = \frac{x}{a}, \quad \frac{\partial\phi}{\partial\eta} = \frac{y}{a}. \tag{8}$$

Letting $\partial/\partial\ell$ denote differentiation with respect to arc length around the boundary of Figure 3 in a counter-clockwise sense, boundary values may be computed from

$$\frac{\partial\phi}{\partial\ell} = \frac{\partial\phi}{\partial\xi}\,\frac{\partial\xi}{\partial\ell} + \frac{\partial\phi}{\partial\eta}\,\frac{\partial\eta}{\partial\ell} = \mathrm{Re}\left\{\left(\frac{x - iy}{a}\right)\frac{\partial\zeta}{\partial\ell}\right\}. \tag{9}$$

This is readily shown, from stress boundary conditions and coordinates of Figure 1, to vanish on the inclined radial lines BC and EF and on the circular arc CDE. Since $\partial\zeta/\partial\ell = \pm 1$ on the top and bottom sides of the slit, respectively, $\partial\phi/\partial\ell = \pm\, x/a$ on the slit. Integrating and arbitrarily setting $\phi(1,0) = 0$, one obtains for boundary values $\phi = 0$ on the inclined radial lines and circular arc, and on both top and bottom sides of the slit

$$\phi(\xi,0) = -\xi, \quad 0 < \xi < s \tag{10}$$

$$\phi(\xi,0) = -\beta s + (\beta - 1)\,\xi, \quad s < \xi < \delta \tag{11}$$

where

$$\beta = b/a \tag{12}$$

is the dimensionless ratio of plane width to notch depth.

Since $x - iy = R(\theta)e^{-i\theta}$ on the elastic-plastic boundary, the position of the boundary may be determined from (3) as

$$\frac{R(\theta)}{a} = e^{i\theta}\,f'(e^{i\theta})$$

$$\frac{R_o}{a} = f'(1) \tag{13}$$

Equation (2) may be integrated to give displacements (referred to polar

coordinates) of the elastic-plastic boundary. Setting $w[R_o, 0] = 0$,

$$w[R(\theta), \theta] = \frac{k}{G}\int_o^\theta R(\theta)d\theta = \frac{-ka}{G} i\int_1^{e^{i\theta}} f'(e^{i\theta})d(e^{i\theta}),$$

and thus

$$\frac{Gw[R(\theta), \theta]}{ka} = -i[f(e^{i\theta}) - f(1)]$$

$$\frac{Gw_o}{ka} = -i[f(e^{i\pi/2 - i\alpha}) - f(1)], \tag{14}$$

where $w_o$ is the displacement discountinuity occuring at the notch tip.

## SOLUTION OF PROBLEM

The problem of Figure 3 is readily solved by resort to conformal mapping onto a unit semi-circle in the complex $\Omega = \omega + i\lambda$ plane, with corresponding points shown in Figure 4, where

$$\Omega = \Omega(\zeta) = i\left(\frac{\zeta^n - \delta^n}{1 - \zeta^n\delta^n}\right)^{1/2}, \tag{15}$$

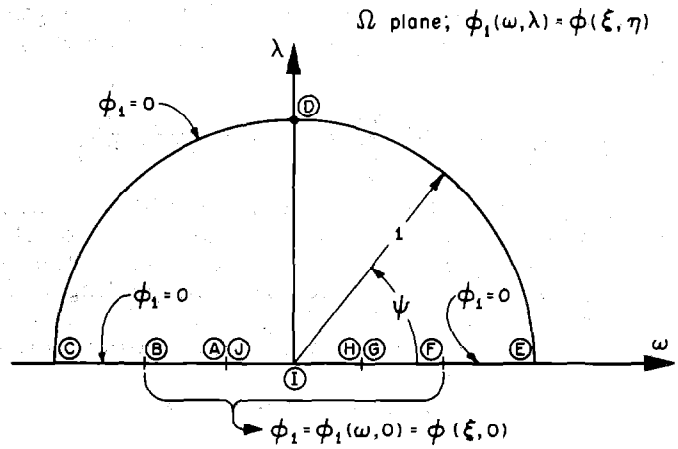


Fig. 4. Map of stress plane onto unit semi-circle

and the exponent n is given in terms of notch angle $\alpha$ by

$$n = \frac{2\pi}{\pi - 2\alpha}. \tag{16}$$

Let $\phi_1(\omega, \lambda) = \phi(\xi, \eta)$ so that $\phi_1(\omega, \lambda) = \mathrm{Re}\{f(\zeta)\}$ when $\zeta$ is expressed in terms of $\Omega$. Boundary conditions are as in Figure 4 with $\phi_1$ vanishing everywhere except on the segment BIF of the $\omega$ axis. The function

$$g(\Omega) = \frac{1}{\pi i}\int_{BIF} \frac{\phi_1(\omega, 0)d\omega}{\omega - \Omega} \tag{17}$$

has a real part equal to $\phi_1(\omega, 0)$ on BIF and vanishing everywhere else on the $\omega$ axis (in fact, $g(\Omega)$ is the solution for the half plane problem with

identical boundary values on the $\omega$ axis). A solution to the unit semi-circle problem of Figure 4 is now obtained by adding to $g(\Omega)$ another analytic function having a real part which (a) vanishes on the $\omega$ axis for $|\omega| < 1$ since $g(\Omega)$ already satisfies prescribed conditions, and (b) is equal to $-\mathrm{Re}\{g(\Omega)\}$ on the unit circle $\Omega = e^{i\psi}$ so as to satisfy $\phi_1 = 0$ for $|\Omega| = 1$. Consider

$$g(1/\Omega) = \frac{1}{\pi i} \int_{BIF} \frac{\phi_1(\omega, 0)d\omega}{\omega - 1/\Omega}, \tag{18}$$

which is analytic and free of branch cuts for all $|\Omega| \leq 1$. Clearly, for $\Omega$ on the real axis between $\pm 1$, $g(1/\Omega)$ is pure imaginary so that condition (a) is satisfied. Since $\overline{g(\Omega)} = -g(\overline{\Omega})$ and $\overline{\Omega} = e^{-i\psi} = 1/\Omega$ on the unit circle,

$$\mathrm{Re}\{g(1/\Omega)\} = \frac{1}{2}\left[g(1/\Omega) + \overline{g(1/\Omega)}\right] = \frac{1}{2}\left[g(1/\Omega) - g(\Omega)\right]$$

$$= -\frac{1}{2}\left[g(\Omega) + \overline{g(\Omega)}\right] = -\mathrm{Re}\{g(\Omega)\},$$

satisfying condition (b). Thus $\phi_1(\omega, \lambda) = \mathrm{Re}\{g(\Omega) + g(1/\Omega)\}$ is the solution and $f(\zeta) = g\left[\Omega(\zeta)\right] + g\left[1/\Omega(\zeta)\right]$ leading to

$$f(\zeta) = \frac{1}{\pi i} \int_{BIF} \phi_1(\omega, 0) \left[\frac{1}{\omega - \Omega(\zeta)} + \frac{1}{\omega - 1/\Omega(\zeta)}\right] d\omega$$

$$= \frac{1}{\pi i} \int_{IF} \phi_1(\omega, 0) \left[\frac{1}{\omega - \Omega(\zeta)} + \frac{1}{\omega - 1/\Omega(\zeta)}\right.$$

$$\left. - \frac{1}{\omega + \Omega(\zeta)} - \frac{1}{\omega + 1/\Omega(\zeta)}\right] d\omega, \tag{19}$$

since $\phi_1(\omega, 0)$ is an even function.

Transforming the integral in the $\Omega$ plane to an integral in the $\zeta$ plane, combining fractional terms, and setting $\phi_1(\omega, 0) = \phi(\xi, 0)$ of (10, 11),

$$f(\zeta) = -\frac{2}{\pi i} \Omega(\zeta)\left[1+\Omega^2(\zeta)\right] \int_0^{\delta} \frac{\phi(\xi, 0)\omega'(\xi)\left[\omega^2(\xi)-1\right] d\xi}{\Omega^2(\zeta)\omega^4(\xi) - \left[1+\Omega^4(\zeta)\right]\omega^2(\xi)+\Omega^2(\zeta)}, \tag{20}$$

with

$$\omega(\xi) = \sqrt{\frac{\delta^n - \xi^n}{1 - \xi^n \delta^n}}. \tag{21}$$

The derivative $f'(\zeta) = (x-iy)/a$ may be determined by first integrating (20) by parts and then differentiating. With $\phi'(\xi, 0) = \frac{\partial \phi(\xi, 0)}{\partial \xi}$, there results

$$f'(\zeta) = \frac{2}{\pi i} \Omega'(\zeta)\left[1 - \Omega^2(\zeta)\right] \int_0^{\delta} \frac{\phi'(\xi, 0)\omega(\xi)\left[1+\omega^2(\xi)\right] d\xi}{\Omega^2(\zeta)\omega^4(\xi) - \left[1+\Omega^4(\zeta)\right]\omega^2(\xi)+\Omega^2(\zeta)}. \tag{22}$$

Since $\Omega'(\delta)$ is infinite, the condition of boundedness of $f'(\delta)$ requires that the coefficient of $\Omega'(\zeta)$ be zero when $\Omega(\zeta) = \Omega(\delta) \equiv 0$. Thus $\delta$ is the solution of

$$0 = \int_0^{\delta} \phi'(\xi, 0) \frac{1 + \omega^2(\xi)}{\omega(\xi)} d\xi, \tag{23}$$

which with the aid of (10, 11, 21) and the substitution $t = \xi/\delta$ becomes the implicit equation

$$\beta = \frac{\displaystyle\int_0^1 \frac{1 - \delta^n t^n}{\sqrt{(1 - \delta^{2n} t^n)(1 - t^n)}}\, dt}{\displaystyle\int_{s/\delta}^1 \frac{1 - \delta^n t^n}{\sqrt{(1 - \delta^{2n} t^n)(1 - t^n)}}\, dt} \tag{24}$$

When the plane of Figure 1 is infinitely wide so that $\beta \longrightarrow \infty$, one has $\delta = s$ and the boundedness condition is no longer required. The above solutions for $f(\zeta)$ and $f'(\zeta)$ remain valid except that now $\delta$ is everywhere replaced by $s$ and $\phi_1(\xi, 0)$ is given by (10) with (11) being disregarded.

## ELASTIC-PLASTIC BOUNDARY

The location and displacements of the elastic-plastic boundary are determined by (13) and (14) when $\zeta = e^{i\theta}$. Comparing Figures 3 and 4, points on the arc of unit circle in the $\zeta$ plane are seen to map onto an arc of unit circle in the $\Omega$ plane so that $\Omega(e^{i\theta}) = e^{i\psi(\theta)}$ and $\Omega'(e^{i\theta}) = -ie^{-i\theta} \frac{d}{d\theta} \Omega(e^{i\theta}) = \psi'(\theta) e^{-i\theta} e^{i\psi(\theta)}$. One readily shows that

$$\psi(\theta) = \frac{\pi}{2} + \frac{1}{2} \cos^{-1} \left\{ \frac{(1 + \delta^{2n}) \cos n\theta - 2\delta^n}{(1 + \delta^{2n}) - 2\delta^n \cos n\theta} \right\}, \tag{25}$$

where that branch of the inverse cosine is chosen which varies from 0 when $\theta = 0$ to $\pi$ when $\theta = \pi/n = 1/2\ \pi - \alpha$, and

$$\psi'(\theta) = \frac{n}{2} \frac{1 - \delta^{2n}}{(1 + \delta^{2n}) - 2\delta^n \cos n\theta}\ . \tag{26}$$

With the above substitutions for $\Omega(e^{i\theta})$ and $\Omega'(e^{i\theta})$ inserted into (22), equation (13) results in

$$\frac{R(\theta)}{a} = -\frac{4}{\pi} \psi'(\theta) \sin\left[\psi(\theta)\right] \int_0^{\delta} \frac{\phi'(\xi, 0)\, \omega(\xi) \left[\omega^2(\xi) + 1\right] d\xi}{\omega^4(\xi) - 2\omega^2(\xi) \cos\left[2\psi(\theta)\right] + 1}\ . \tag{27}$$

Using previously given expressions for all quantities involved and making the substitution $t = \xi/\delta$, the elastic plastic boundary is given by

$$\frac{R(\theta)}{a} = \frac{2n}{\pi} \frac{\delta^{1 + n/2} \cos \frac{n\theta}{2}}{\sqrt{1 - 2\delta^n \cos n\theta + \delta^{2n}}} \left[ \int_0^1 - \beta \int_{s/\delta}^1 \right] \left[ \frac{(1 - \delta^n t^n) \sqrt{(1 - t^n)(1 - \delta^{2n} t^n)}}{1 - 2\delta^n t^n \cos n\theta + \delta^{2n} t^{2n}} \right] dt\ . \tag{28}$$

for $-(\pi/2-\alpha) < \theta < +(\pi/2-\alpha)$. Setting $\theta = 0$, the maximum zone $R_o$ is

$$\frac{R_o}{a} = \frac{2n}{\pi} \frac{\delta^{1+n/2}}{1-\delta^n} \left[ \int_0^1 - \beta \int_{s/\delta}^1 \right] \left[ \frac{\sqrt{(1-t^n)(1-\delta^{2n}t^n)}}{1-\delta^n t^n} \right] dt \,. \tag{29}$$

Since $f(1) = 0$ equation (14) leads, through (20) and the expression $\Omega(e^{i\theta}) = e^{i\psi(\theta)}$, to

$$\frac{Gw\,[R(\theta),\theta]}{ka} = \frac{4}{\pi} \cos\left[\psi(\theta)\right]$$

$$\int_0^\delta \frac{\phi(\xi,0)\ \omega'(\xi)\left[\omega^2(\xi)-1\right]\ d\xi}{\omega^4(\xi) - 2\omega^2(\xi)\cos\left[2\psi(\theta)\right] + 1} \,. \tag{30}$$

Substituting as for (28) above and carrying out part of the integration, displacements of points along the elastic plastic boundary become

$$\frac{Gw\,[R(\theta),\theta]}{ka}$$

$$= \frac{\beta s}{\pi} \log \left[ \frac{(1-s^n)\sqrt{1-2\delta^n\cos n\theta + \delta^{2n}} + 2\sin\left(\frac{n\theta}{2}\right)\sqrt{(\delta^n-s^n)(1-s^n\delta^n)}}{(1-s^n)\sqrt{1-2\delta^n\cos n\theta + \delta^{2n}} - 2\sin\left(\frac{n\theta}{2}\right)\sqrt{(\delta^n-s^n)(1-s^n\delta^n)}} \right]$$

$$+ \frac{2n}{\pi} \delta^{1+n/2} \sqrt{1-2\delta^n\cos n\theta + \delta^{2n}}\ \sin\frac{n\theta}{2} \left[ \int_0^1 - \beta \int_{s/\delta}^1 \right]$$

$$\left[ \frac{t^n(1+\delta^n t^n)}{\sqrt{(1-t^n)(1-\delta^{2n}t^n)}\ (1-2\delta^n t^n\cos n\theta + \delta^{2n}t^{2n})} \right] dt \,, \tag{31}$$

for $-(\pi/2-\alpha) < \theta < +(\pi/2-\alpha)$. When $\theta = \pm(\pi/2-\alpha)$, $R(\theta) = 0$ but the displacement is finite. Thus there is a displacement discountinuity of magnitude $2w_o$ at the notch tip where $w_o$, the displacement at $\theta = (\pi/2-\alpha)$, is

$$\frac{Gw_o}{ka} = \frac{2\beta s}{\pi} \log \left[ \frac{\sqrt{1-s^n\delta^n} + \sqrt{\delta^n - s^n}}{\sqrt{1-s^n\delta^n} - \sqrt{\delta^n - s^n}} \right]$$

$$+ \frac{2n}{\pi} \delta^{1+n/2}(1+\delta^n) \left[ \int_0^1 - \beta \int_{s/\delta}^1 \right]$$

$$\left[ \frac{t^n}{\sqrt{(1-t^n)(1-\delta^{2n}t^n)}\ (1+\delta^n t^n)} \right] dt \,. \tag{32}$$

Equations (28, 29, 31, 32) remain valid for a plane of infinite width ($\beta = \infty$), except that now $\delta$ is everywhere replaced by s, the logarithmic terms in (31, 32) are omitted, and the integral operator

$$\int_0^1 - \beta \int_{s/\delta}^1 \text{ is replaced by } \int_0^1 .$$

## SMALL SCALE YIELDING

At low stress levels the plastic zone size is small compared to all geometric dimensions of Figure 1. Appropriate small scale yielding solutions are then derived from formulae of the last sections by neglecting terms of order $\delta, s$ in comparison to unity. Equation (24) for the determination of $\delta$ becomes

$$\beta \int_{s/\delta}^{1} \frac{dt}{\sqrt{1 - t^n}} = \int_{o}^{1} \frac{dt}{\sqrt{1 - t^n}} = \frac{\sqrt{\pi}}{n} \frac{\Gamma(1/n)}{\Gamma(\frac{2 + n}{2n})} , \tag{33}$$

where $\Gamma(x) = \int_o^\infty r^{x-1} e^{-r} dr$ is the Gamma function. One may show that the ratio of $s/\delta = \tau/\tau_i$ resulting from (33) is the same as the ratio in an elastic solution of the problem of Figure 1. With the aid of (33) equations (29), (28), and (31) result, for small values of s and $\delta$, in

$$\frac{R_o}{a} = \frac{4n\beta}{\pi(2 + n)} \sqrt{(\delta/s)^n - 1} \; s^{1 + n/2} \tag{34}$$

$$R(\theta) = R_o \cos \frac{n\theta}{2}, \quad w\left[R(\theta), \theta\right] = \frac{2k}{nG} R_o \sin \frac{n\theta}{2} . \tag{35}$$

When $\beta \longrightarrow \infty$, $\delta \longrightarrow s$, and one may show that

$$\int_{s/\delta}^{1} (1 - t^n)^{-1/2} \, dt \longrightarrow 2/n \left[1 - (s/\delta)^n\right]^{+1/2} \longrightarrow 2/n \left[(\delta/s)^n - 1\right]^{1/2} .$$

Then, using (33), equation (34) becomes

$$\frac{R_o}{a} = \frac{2n}{\sqrt{\pi}\,(2+n)} \frac{\Gamma(\frac{1}{n})}{\Gamma(\frac{2+n}{2n})} \; s^{1+n/2} , \tag{36}$$

for the maximum plastic zone size with small scale yielding near a notch in a plane of infinite width. This may also be derived directly through the formalism described above when $\beta = \infty$. After some identities involving Gamma functions, the limiting case of (36) is seen to agree with the results of McClintock and Hult.[4]

## SOLUTION AT LIMIT LOAD

When $\delta = \tau/k = 1$ the yield zone completely traverses the plane of Figure 1 and the limit load has been achieved. By overall equilibrium, this occurs when $\tau b = k(b-a)$ or $s = 1 - 1/\beta$. Rather than attempt a difficult limiting process, the solution for $\delta = 1$ is obtained directly. The upper part of the $\zeta$ plane of Figure 3 is reproduced with appropriate boundary conditions in Figure 5(a) and mapped onto the unit semi-circle in the $\zeta^{2n}$ plane of Figure 5(b). Following the same procedure which led to the solution (19) for the Dirichlet problem of a unit semi-circle, $f(\zeta)$ is given by

$$f(\zeta) = \frac{n}{\pi i} \int_o^1 t^{n-1} \, \phi(t, 0) \left[\frac{1}{t^n - \zeta^n} + \frac{1}{t^n - \zeta^{-n}}\right] dt , \tag{37}$$

with $\phi(t, 0) = -t$, $0 < t < 1 - 1/\beta$, and $\phi(t, 0) = -(\beta-1)(1-t)$, $1 - 1/\beta < t < 1$.

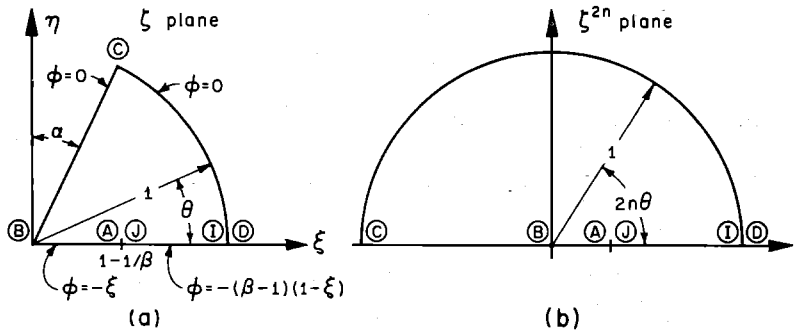


Fig. 5. (a) Upper half of $\zeta$ plane and (b) Its map onto unit semi-circle, for limit load conditions

The position of the elastic plastic boundary at limit load may now be found from (13). There results

$$\frac{R(\theta)}{a} = \frac{2n}{\pi} \sin n\theta \left[ (\beta-1) \int_{1-1/\beta}^{1} - \int_{0}^{1-1/\beta} \right] \left[ \frac{t^n}{1-2t^n \cos n\theta + t^{2n}} \right] dt, \quad (38)$$

and one may verify that $R_o/a = (\beta-1)$ as expected. Displacements when yielding completely traverses the plane are, from (14),

$$\frac{Gw\,[R(\theta),\theta]}{ka} = \frac{4n}{\pi} \sin^2 \frac{n\theta}{2} \left\{ \int_{0}^{1-1/\beta} \frac{t^n(1+t^n)\,dt}{(1-t^n)(1-2t^n \cos n\theta + t^{2n})} \right.$$

$$\left. + (\beta-1) \int_{1-1/\beta}^{1} \frac{t^{n-1}(1-t)(1+t^n)\,dt}{(1-t^n)(1-2t^n \cos n\theta + t^{2n})} \right\}, \quad (39)$$

with the notch opening displacement $w_o$ given by

$$\frac{Gw_o}{ka} = \frac{4n}{\pi} \left\{ \int_{0}^{1-1/\beta} \frac{t^n\,dt}{(1-t^n)(1+t^n)} + (\beta-1) \int_{1-1/\beta}^{1} \frac{t^{n-1}(1-t)\,dt}{(1-t^n)(1+t^n)} \right\}. \quad (40)$$

The displacements of (39) and (40), are those occurring at the instant when the plastic zone reaches the free boundary of Figure 1. Within the context of perfect plasticity theory,[12] unlimited further flow occurs under the fixed limit stress $s = 1 - 1/\beta$. One may show by upper and lower bound theorems that this further flow occurs by discountinuous sliding along the plane formed by the x and z axes of Figure 1, with the position of the elastic-plastic boundary remaining as given by (38) and displacements as given by (39, 40) with a term added to account for the rigid body displacement, due to limit deformation, of the region $y > 0$ with respect to the region $y < 0$.

## SMALL SCALE YIELDING NEAR CRACKS

Many of the solutions given above take simpler forms when $\alpha = 0$ (and from (16), $n = 2$) so that the notch of Figure 1 becomes a crack of length a. Setting $n = 2$, equation (33) relating s to $\delta$ when both are $\ll_1$, as in

the case of small scale yielding, results in

$$s/\delta = \cos \pi/2\beta \ . \tag{41}$$

Substituting into (34, 35) one obtains

$$R_o = \frac{2\beta}{\pi} \tan\left[\frac{\pi}{2\beta}\right] s^2 a \ ; \quad R(\theta) = R_o \cos\theta \tag{42}$$

$$w_o = \frac{k}{G} R_o \ ; \qquad w\left[R(\theta), \theta\right] = w_o \sin\theta \ . \tag{43}$$

The plastic zone as given by (42) is a circular region of diameter $R_o$ ahead of the crack and when $\beta \longrightarrow \infty$ is in agreement with that of [4] for small scale yielding near a crack in a plane of infinite width. It is interesting to note that $K_w = \tau(2\beta a \tan \frac{\pi}{2\beta})^{\frac{1}{2}}$ is the stress intensity factor[13,14] in warping, in the sense that the elastic solution has a singular term of the form $K_w(2\pi x)^{-\frac{1}{2}}$ in the expression for $\tau_{yz}(x, 0)$. Thus (42) for $R_o$ may be written in the alternate form $R_o = K_w^2/(\pi k^2)$ so that, in agreement with [3, 7], the plastic deformation near the crack tip depends on applied loads and geometry only through the elastic stress intensity factor when the scale of yielding is small.

The subject of small scale yielding for cracks under longitudinal shear may be treated in an alternate way which establishes the generality of dependence on elastic stress intensity factors. With proper interpretation of the branch cut, one may show[13] that elastic stress solutions for cracks under symmetrical longitudinal shear loadings always take the form

$$\tau_{yz} - i\tau_{xz} = \frac{K_w}{\sqrt{2\pi}\ (x - iy)^{1/2}} \tag{44}$$

near the crack tip $x = y = 0$; other terms giving vanishing stress at the crack tip must be added for a complete solution. As an approximation valid for small scale yielding, one may then ask for the elastic-plastic solution for an infinite plane with semi-infinite crack along the negative x axis with the boundary conditions that the elastic solution of (44) is approached asymptotically as $|x-iy| \longrightarrow \infty$. Introducing $\zeta = -i(\tau_{xz} + i\tau_{yz})/k$, the (x, y) plane and corresponding $\zeta$ plane are shown in Figures 6(a) and (b) respectively.

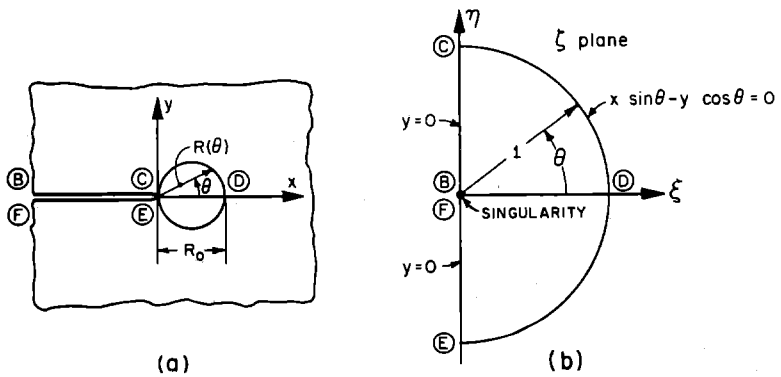


Fig. 6. (a) Physical plane and (b) Stress plane for small scale yielding near cracks

Solving for x-iy (44), the asymptotic boundary condition becomes

$$x\text{-}iy \longrightarrow \frac{K_w^2}{2\pi k^2 \zeta^2} \quad \text{as} \quad \zeta \longrightarrow 0 \ . \tag{45}$$

Noting that boundary conditions in the $\zeta$ plane may be expressed as shown in Figure 6(b), one easily verifies that the correct solution with the singularity as indicated by (45) at $\zeta = 0$ is

$$x\text{-}iy = \frac{K_w^2}{2\pi k^2}\left(1 + \frac{1}{\zeta^2}\right) \ . \tag{46}$$

On the elastic-plastic boundary $x\text{-}iy = R(\theta)e^{-i\theta}$ and $\zeta = e^{i\theta}$ so that for small scale yielding,

$$R_o = \frac{K_w^2}{\pi k^2} \ ; \ R(\theta) = R_o \cos\theta \ , \tag{47}$$

which is identical to the special case of (42) when the appropriate value is inserted for the elastic stress intensity factor $K_w$. Solving for $\zeta$ from (46), stresses in elastic material are given by

$$\tau_{yz} - i\tau_{xz} = \frac{K_w}{\sqrt{2\pi}\left(x - \frac{K_w^2}{2\pi k^2} - iy\right)^{1/2}} \ . \tag{48}$$

Thus, as noted in [15], stresses in elastic material for small scale yielding are identical to those computed from an elastic solution for a crack with its tip at $x = \frac{1}{2} K_w^2/(\pi k^2)$ = one half of the plastic zone diameter.

## LIMIT SOLUTION FOR CRACKS

The solution at limit load (that is, when the dimensionless applied stress $s = 1\text{-}1/\beta$) for cracks is readily computed from the general solutions of equations (38-40) by setting $n = 2$. The resulting expression for the elastic-plastic boundary when yield completely traverses the plane is

$$\frac{R(\theta)}{a} = \left\{(\beta\text{-}1) - \frac{2\beta}{\pi}\tan^{-1}\left[\frac{2\beta(\beta\text{-}1)\sin\theta}{2\beta - 1}\right]\right\}\cos\theta$$

$$+ \frac{2}{\pi}\left\{\frac{\beta}{2}\log\left[\frac{\beta^2 + 2\beta(\beta - 1)\cos\theta + (\beta - 1)^2}{\beta^2 - 2\beta(\beta - 1)\cos\theta + (\beta - 1)^2}\right]\right.$$

$$\left. - (\beta - 1)\log\left[\operatorname{ctn}(\theta/2)\right]\right\}\sin\theta \ , \tag{49}$$

with, as required physically,

$$R_o = a(\beta - 1) = b - a \ . \tag{50}$$

For a crack in a plane of infinite width, $\beta = \infty$ and the limit load is $s = 1$ (or $\tau = k$). It is then seen from (50) that the plastic zone is of infinite

extent in the x direction; however, the zone extends over a length of finite extent in the y direction. This is seen by expanding $R(\theta)$ in a series in $\beta$ and dropping all terms of order $1/\beta$. For $\theta \neq 0$ terms linear in $\beta$ cancel and there results for the elastic-plastic boundary at limit load in a plane of infinite width

$$\frac{R(\theta)}{a} = \frac{2}{\pi}\left\{\sin\theta \log\left[\operatorname{ctn}(\theta/2)\right] + \operatorname{ctn}\theta\right\} - \cos\theta \,. \tag{51}$$

The y coordinate of points on the boundary is $R(\theta)\sin\theta$. Letting $\theta \longrightarrow 0$ is equivalent to $x \longrightarrow \infty$, and $R(\theta)\sin\theta = y \longrightarrow 2a/\pi$, so that the elastic-plastic boundary at limit load has a thickness in the y direction which approaches $4a/\pi$ asymptotically.

Displacements of points on the elastic-plastic boundary at limit load are from (39) with $n = 2$

$$\frac{\pi G w\left[R(\theta),\theta\right]}{2\,k\,a} = 2(\beta-1)\left\{\frac{\cos\theta}{2}\log\left[\frac{4\beta^2\cos^2(\theta/2)}{\beta^2+2\beta(\beta-1)\cos\theta+(\beta-1)^2}\right]\right.$$

$$\left. + \sin\theta\tan^{-1}\left[\frac{\tan(\theta/2)}{2\beta-1}\right]\right\} + (\beta-1)\left\{-\sin^2(\theta/2)\log\left[\frac{\beta^4-2\beta^2(\beta-1)^2\cos 2\theta+(\beta-1)^4}{4\beta^4\sin^2\theta}\right]\right.$$

$$\left. + \sin\theta\tan^{-1}\left[\frac{(2\beta-1)\operatorname{ctn}\theta}{\beta^2+(\beta-1)^2}\right]\right\} - \left\{\frac{\cos\theta}{2}\log\left[\frac{\beta^2+2\beta(\beta-1)\cos\theta+(\beta-1)^2}{\beta^2-2\beta(\beta-1)\cos\theta+(\beta-1)^2}\right]\right.$$

$$\left. + \sin\theta\tan^{-1}\left[\frac{2\beta(\beta-1)\sin\theta}{2\beta-1}\right]\right\} + (2\beta-1)\log(2\beta-1) - 2(\beta-1)\log(2\beta) \,. \tag{52}$$

The crack opening displacement $w_o$ at limit load may be obtained from (52) by setting $\theta = \pi/2$ or directly from (40). There results

$$w_o = \frac{ka}{G}\left\{(\beta-1) + \frac{2}{\pi}\log(2\beta-1) - \frac{4}{\pi}\beta\tan^{-1}\left(\frac{\beta-1}{\beta}\right)\right.$$

$$\left. - \frac{2}{\pi}(\beta-1)\log\left(\frac{4\beta^2-4\beta+2}{4\beta^2-4\beta+1}\right)\right\} . \tag{53}$$

For large $\beta$ linear terms cancel and neglecting all terms of order unity, the crack opening displacement at limit load behaves as

$$w_o \longrightarrow \frac{2\,k\,a}{\pi\,G}\log(2\beta) \text{ as } \beta \longrightarrow \infty \,. \tag{54}$$

## GENERAL CASE OF CRACKS

Results of the last two sections are for small scale yielding and for limit load yielding around cracks. For the general case of cracks solutions valid at all load levels are obtained in terms of elementary functions and the elliptic functions of first and second kind

$$E_1(\mu,x) = \int_0^x \frac{dt}{\sqrt{(1-t^2)(1-\mu^2t^2)}} \quad ; \quad E_2(\mu,x) = \int_0^x \sqrt{\frac{1-\mu^2t^2}{1-t^2}}\,dt \,. \tag{55}$$

Equation (24) which determines the unknown parameter $\delta = \tau_I/k$ in terms of $s = \tau/k$ and $\beta = b/a$ takes the form

$$\beta = \frac{E_2(\delta^2, 1) - (1-\delta^2)\, E_1(\delta^2, 1)}{\left[E_2(\delta^2, 1) - E_2(\delta^2, s/\delta)\right] - (1-\delta^2)\left[E_1(\delta^2, 1) - E_1(\delta^2, s/\delta)\right]} \quad . \tag{56}$$

The implicit nature of this equation causes some difficulty for the effective determination of $\delta$. Therefore, graphs of $\delta$ in terms of the dimensionless net-section stress (that is, average stress on uncracked portion of x axis) $\tau_n/k = (1-a/b)^{-1}\tau/k$, as obtained from computer calculation, are given for various values of the crack length to plane width ratio, a/b, in Figure 7.

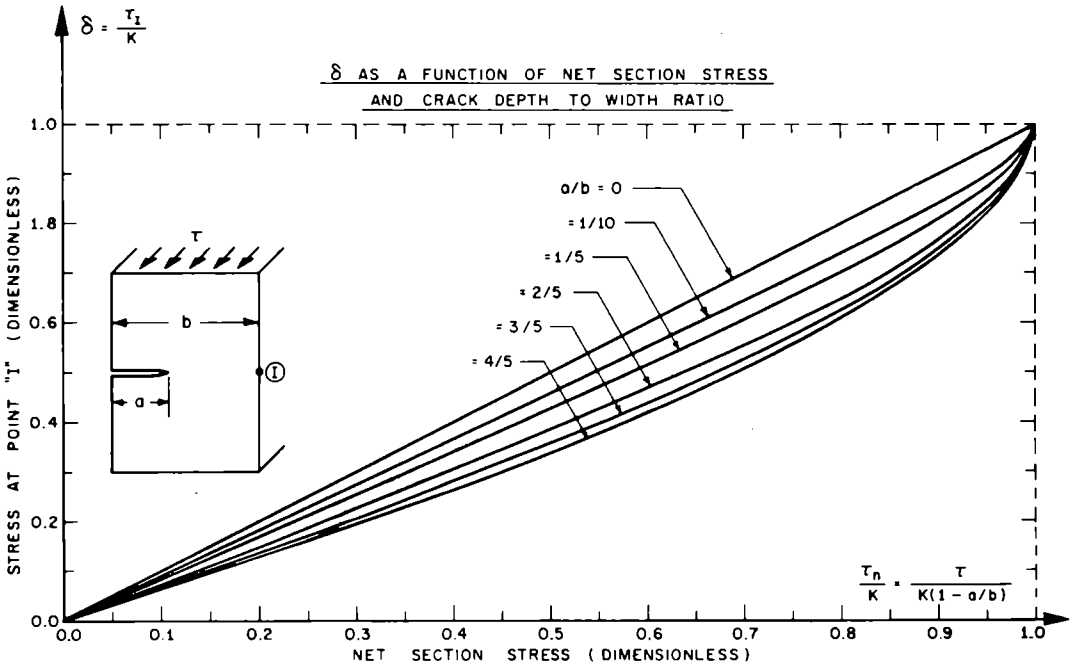


Fig. 7

Equations for the position of the elastic-plastic boundary and corresponding displacements may be written in terms of elliptic functions; these, however, involve the generally untabulated functions of the third kind with a complex parameter, and are therefore more readily computed directly from the single integrals of (28) and (31) with $n = 2$ and $\delta$ as determined from (56). Of more direct physical interest are the maximum plastic zone size $R_o$ and crack opening displacement $w_o$ which fortunately involve only the tabulated elliptic functions of (55).

Setting $n = 2$ in (29) and using (56) to simplify, there results for the maximum zone size

$$\frac{R_o}{a} = (\beta-1) - \frac{2}{\pi}\left[(\beta-1)\, E_2(\delta^2, 1) - \beta E_2(\delta^2, s/\delta)\right]$$

$$- \frac{2}{\pi}\beta \tan^{-1}\left[\frac{1-\delta^2}{\sqrt{(1-\delta^2 s^2)(\delta^2 s^{-2}-1)}}\right] \quad . \tag{57}$$

When $\beta = \infty$ one may find $R_o$ by the formalism given earlier or by inserting (56) into (57) and appropriate limiting. There results for the maximum plastic zone size in a cracked plane of infinite width

$$R_o = a \left\{ -1 + \frac{4}{\pi} \left[ \frac{E_2(s^2,1)}{1-s^2} - \frac{1+s^2}{2} E_1(s^2,1) \right] \right\} . \qquad (58)$$

After some transformations of complete elliptic functions which involve distorting the integration path of (55) to a contour around the branch cut $-1 < t < +1$ and then to a circle of radius $1/s$ in the complex t plane, this becomes

$$R_o = a \left\{ -1 + \frac{2}{\pi} \frac{1+s^2}{1-s^2} E_2\left(\frac{2s}{1+s^2}, 1\right) \right\} , \qquad (59)$$

in agreement with the result obtained by Bilby et al.[16] directly from an integral for $R_o$ given in [4].

The crack opening displacement, $w_o$, is from (32) with $n = 2$

$$\frac{Gw_o}{k\,a} = (\beta-1) - \frac{2}{\pi}(1+\delta^2)\left[(\beta-1)E_1(\delta^2,1) - \beta E_1(\delta^2, s/\delta)\right]$$

$$+ \frac{2\beta s}{\pi} \log\left[\frac{\sqrt{1-s^2\delta^2} + \sqrt{\delta^2-s^2}}{\sqrt{1-s^2\delta^2} - \sqrt{\delta^2-s^2}}\right]$$

$$- \frac{2\beta}{\pi} \tan^{-1}\left[\frac{1+\delta^2}{\sqrt{(1-\delta^2 s^2)(\delta^2 s^{-2}-1)}}\right] \qquad (60)$$

For a plane of infinite width, this becomes

$$w = \frac{ka}{G}\left\{-1 + \frac{2}{\pi}(1+s^2)E_1(s^2,1)\right\} . \qquad (61)$$

Numerical results for the plastic zone size and crack opening displacement are not tabulated here; however, as indicated in the next section, these may be readily obtained from the graphs of Figures 8 to 12 dealing with the application of results to the determination of fracture criteria.

## APPLICATION TO FRACTURE PREDICTION

The preceding sections have given a solution to the elastic-plastic problem of a notched body subjected to a uniform applied stress field, with particular attention to the case of cracks. We now turn to the application of these results in the prediction of the fracture of bodies containing crack-like flaws.

The approach taken here will be, as in [3], to ignore questions as to the details of the process of material separation at the crack tip, and to base a fracture criterion on parameters which describe, according to the continuum solution, the local state of affairs at the crack tip in terms of applied stress and geometrical dimensions. As will be seen subsequently, such an approach is not entirely satisfactory as different measures of the crack tip deformation lead to some discrepancies in resulting fracture criteria.

Consider first a case where the specimen fails at low stress levels with the plastic zone size at fracture negligible in comparison to all geometric dimensions. Such a result may always be forced by choosing a sufficiently (although sometimes impractically) large specimen with a long crack. In this case the results of an earlier section titled "Small Scale Yielding Near Cracks" are appropriate, and it was shown there that the entire local stress and deformation field depended on applied loads and geometry only through the elastic stress intensity factor $K_w = \tau(2\beta a \tan \frac{\pi}{2\beta})^{\frac{1}{2}}$.

Thus small scale yielding fractures occur when $K_w$ reaches some critical value, say $K_w^f$. With the aid of equation (47), the plastic zone size, $R_o^f$, at fracture in a small scale yielding experiment is

$$R_o^f = \frac{1}{\pi} \frac{\left(K_w^f\right)^2}{k^2}, \tag{62}$$

and, from (43), the crack opening displacement at fracture is

$$w_o^f = \frac{k}{G} R_o^f . \tag{63}$$

For the following derivation of failure criteria appropriate when yielding is not on a small scale, it will be convenient to view $R_o^f$, as defined by (62), as a characteristic length describing a given material.

Suppose that fracture occurs when the strain at some point ahead of the crack tip, or the average strain taken over some typical line element ahead of the crack, reaches a critical value. From (2) it is noted that the strain in the plastic zone along points on the x axis is given by $\gamma_{yz}(x, 0) = \frac{k}{G} \frac{R_o}{x}$. Thus such a fracture criterion is equivalent to one based on the achievement of a critical plastic zone size, $R_o$, and from (62), this value is $R_o = R_o^f$. For a given ratio of crack length to plane width, $a/b = 1/\beta$, one may determine $R_o/a$ in terms of the applied stress from (57) (since $\delta$ is known in terms of $a/b$ and $\tau/k$ from (56), or equivalently Figure 7). The crack length corresponding to a given fracture stress and plane width to crack length ratio is found in dimensionless form by setting the left side of (57) equal to $R_o^f/a$. The resulting equations for the dimensionless net section stress at fracture, $\tau_n^f/k$, in terms of dimensionless crack length, $a/R_o^f$, are graphed in Figure 8 for various size ratios $a/b$. Note that if the uncracked plane width, $b-a$, is not greater than $R_o^f$, limit conditions govern the fracture stress as indicated by the horizontal portions of curve in Figure 8 at the net section stress $\tau n/k = 1$. One may determine the range of crack lengths, $a/R_o^f$, corresponding to failure at limit load by observing that $b - a \leq R_o$ implies that $a/R_o^f \leq (b/a - 1)^{-1}$. The fracture criteria of Figure 8 alternately may serve to determine the plastic zone size $R_o$. The ratio $a/R_o^f$ from Figure 8 is equal to $a/R_o$, as given by (57), for the same net stress and $a/b$ ratio.

One may base a fracture criterion on other parameters describing the local deformation. An appealing choice is to suppose fracture occurs when the crack opening displacement, $w_o$, reaches a critical value of $w_o = w_o^f = \frac{k}{G} R_o^f$, according to (63). In terms of strain, $w_o$ represents an average of the non-vanishing strain component $\gamma_{\theta z}$ over a small semi-circular arc near the crack tip in the plastic zone. One may determine the ratio $\frac{Gw_o}{ka}$ from (60); when $w_o = w_o^f$, this is equal to $R_o^f/a$. Therefore, the crack length corresponding to a given fracture stress and plane width to crack length ratio is found in dimensionless form by setting the left side

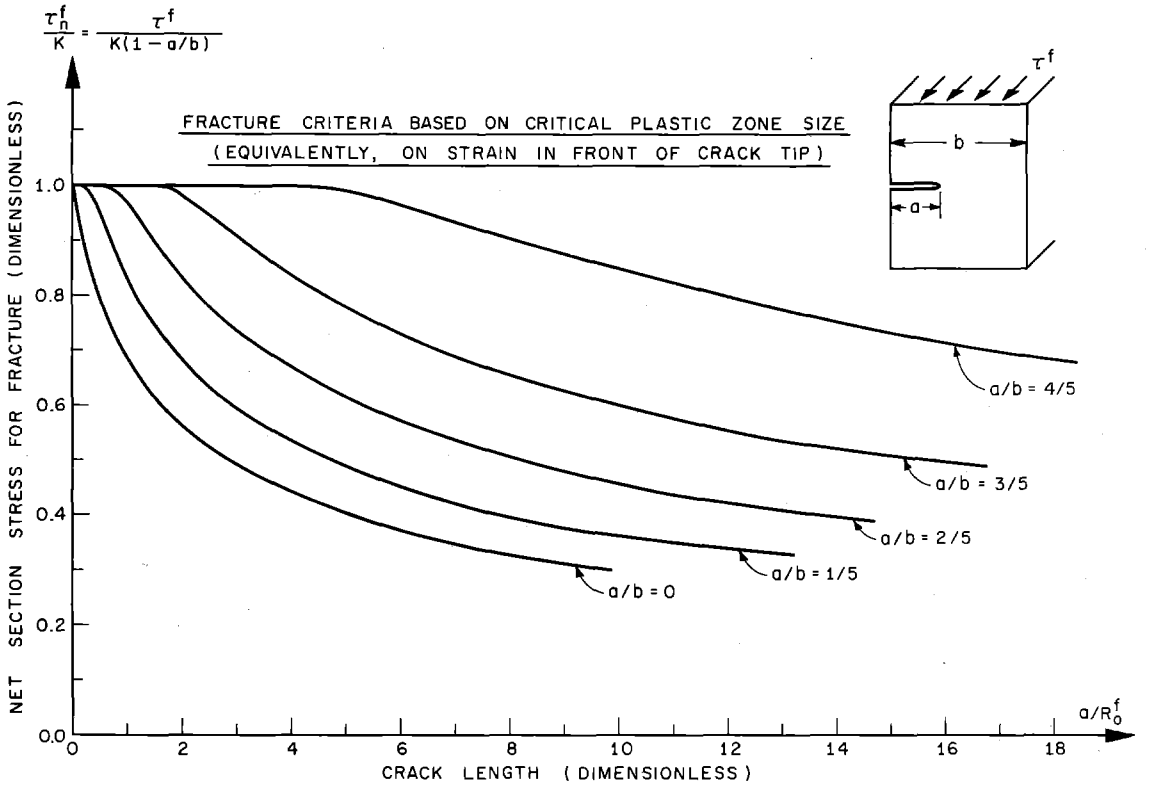
$\frac{\tau_n^f}{K} = \frac{\tau^f}{K(1-a/b)}$
FRACTURE CRITERIA BASED ON CRITICAL PLASTIC ZONE SIZE
(EQUIVALENTLY, ON STRAIN IN FRONT OF CRACK TIP)
$\tau^f$
b
a
a/b = 4/5
a/b = 3/5
a/b = 2/5
a/b = 1/5
a/b = 0
NET SECTION STRESS FOR FRACTURE (DIMENSIONLESS)
1.0
0.8
0.6
0.4
0.2
0.0
0
2
4
6
8
10
12
14
16
18
$a/R_0^f$
CRACK LENGTH (DIMENSIONLESS)

Fig. 8

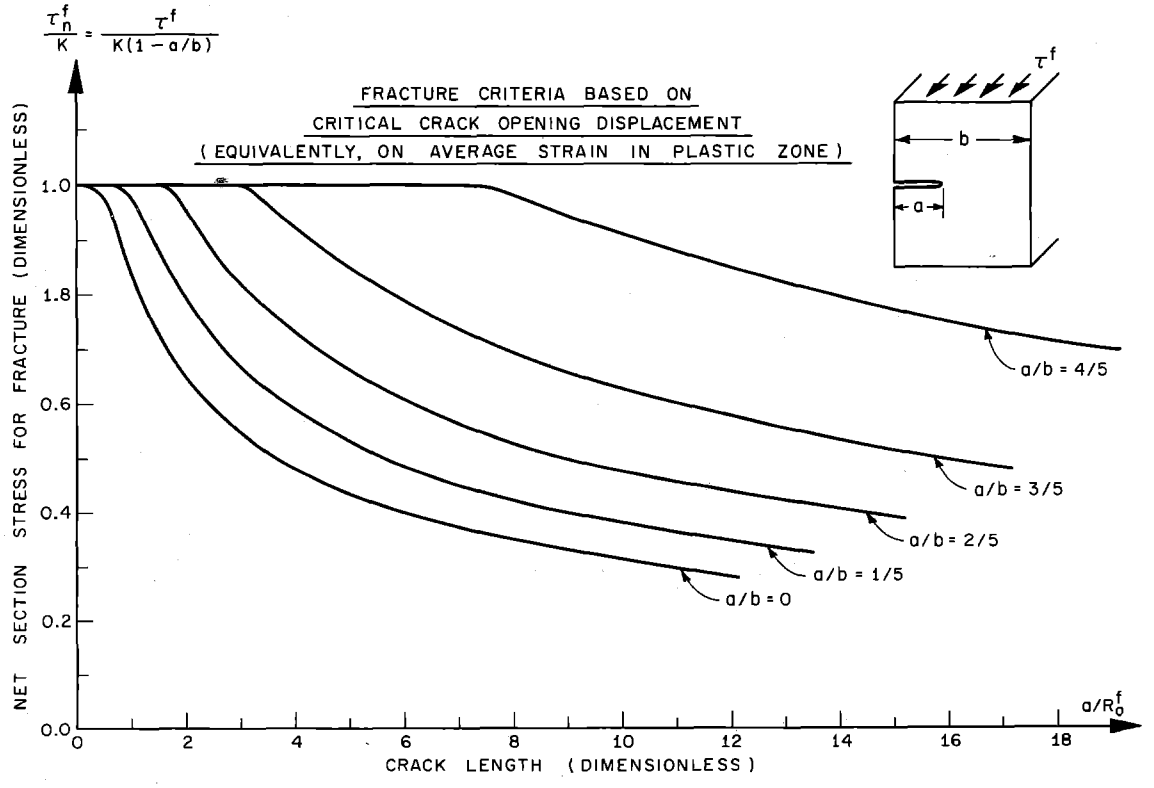
$\frac{\tau_n^f}{K} = \frac{\tau^f}{K(1-a/b)}$
FRACTURE CRITERIA BASED ON
CRITICAL CRACK OPENING DISPLACEMENT
(EQUIVALENTLY, ON AVERAGE STRAIN IN PLASTIC ZONE)
$\tau^f$
b
a
a/b = 4/5
a/b = 3/5
a/b = 2/5
a/b = 1/5
a/b = 0
NET SECTION STRESS FOR FRACTURE (DIMENSIONLESS)
1.0
1.8
0.6
0.4
0.2
0.0
0
2
4
6
8
10
12
14
16
18
$a/R_0^f$
CRACK LENGTH (DIMENSIONLESS)

Fig. 9

of (60) equal to $R_o^f/a$. Resulting equations for the dimensionless net section stress at fracture, $\tau_n/k$, in terms of dimensionless crack length, $a/R_o^f$, are graphed in Figure 9 for various size ratios a/b. In analogy with previous remarks, the horizontal portions of curve at $\tau_n/k = 1$ correspond to cases where the limit load is achieved before the crack opening displacement required for fracture is attained. The crack opening displacement, $w_o$, may be obtained from Figure 9. For a given net section stress and crack length to plane width ratio, the corresponding value of $a/R_o^f$ is equal to $ka/Gw_o$ as given by (60).

The fracture criteria of Figures 8 and 9, based respectively on a critical plastic zone size and a critical crack opening displacement, determine fracture conditions in terms of $R_o^f$, the plastic zone size at fracture in a small scale yielding experiment for which the elastic stress intensity factor essentially controls failure. This need not be determined directly, but instead may be inferred by matching the results of a single experiment with one of the fracture criteria.

The Griffith-Irwin fracture criterion, in the absence of empirical corrections for plastic yielding, is based on the results of an elastic stress analysis, suggesting fracture to occur when the elastic stress intensity factor, $K_w = \tau\,(2\beta a \tan\frac{\pi}{2\beta})^{\frac{1}{2}}$, attains a critical value $K_w = K_w^f$. To facilitate comparison, $K_w^f$ may be expressed in terms of $R_o^f$ by (62) so that the net section stress at fracture is, according to this criterion,

$$\frac{\tau_n^f}{k} = \frac{\left(\frac{\pi a}{2b}\ \mathrm{ctn}\ \frac{\pi a}{2b}\right)^{1/2}}{1 - \frac{a}{b}} \left(\frac{R_o^f}{a}\right)^{1/2} \tag{64}$$

Figures 10, 11, and 12 present a comparison of the Griffith-Irwin, plastic zone size, and crack opening displacement criteria for crack length to

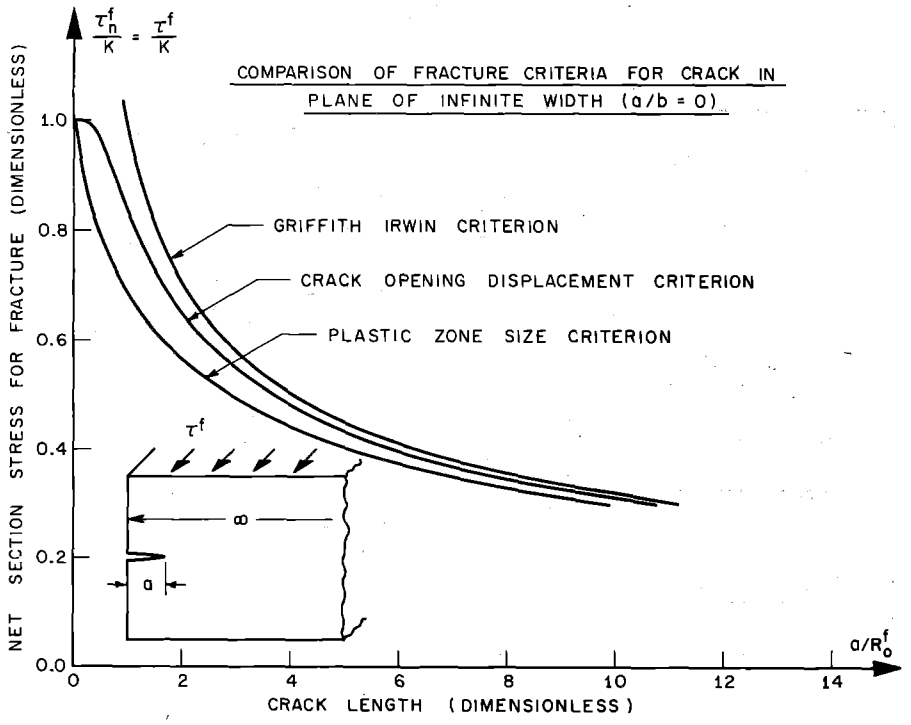


Fig. 10

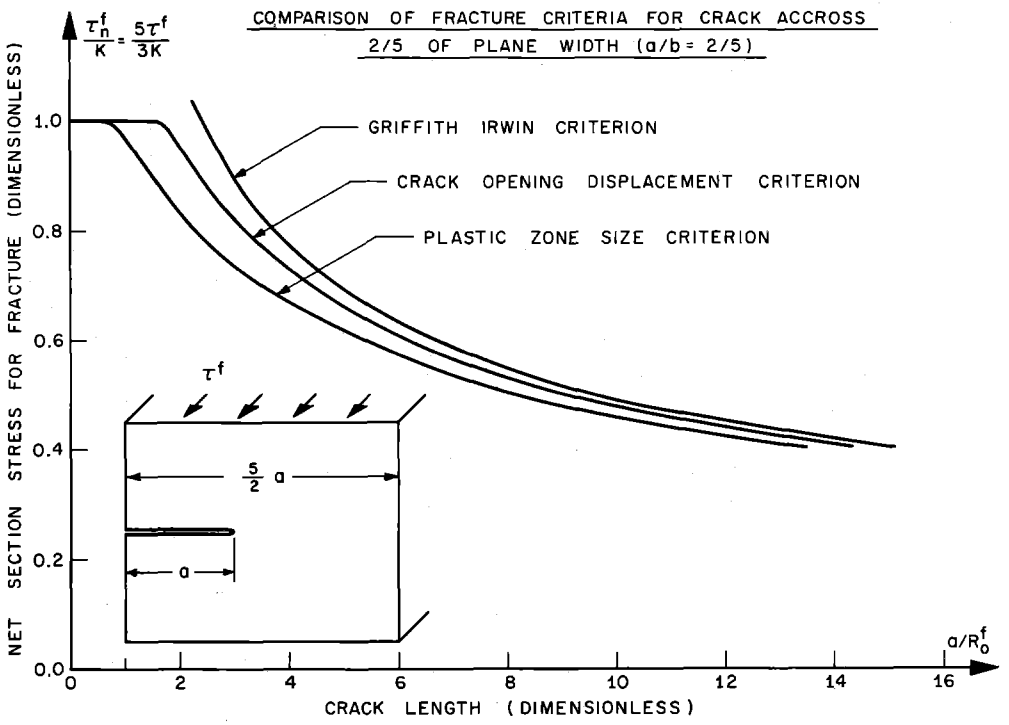
COMPARISON OF FRACTURE CRITERIA FOR CRACK ACCROSS
2/5 OF PLANE WIDTH (a/b = 2/5)
$\frac{\tau_n^f}{K} = \frac{5\tau^f}{3K}$
GRIFFITH IRWIN CRITERION
CRACK OPENING DISPLACEMENT CRITERION
PLASTIC ZONE SIZE CRITERION
$\tau^f$
$\frac{5}{2}$ a
a
NET SECTION STRESS FOR FRACTURE (DIMENSIONLESS)
1.0
0.8
0.6
0.4
0.2
0.0
0
2
4
6
8
10
12
14
16
$a/R_o^f$
CRACK LENGTH (DIMENSIONLESS)

Fig. 11

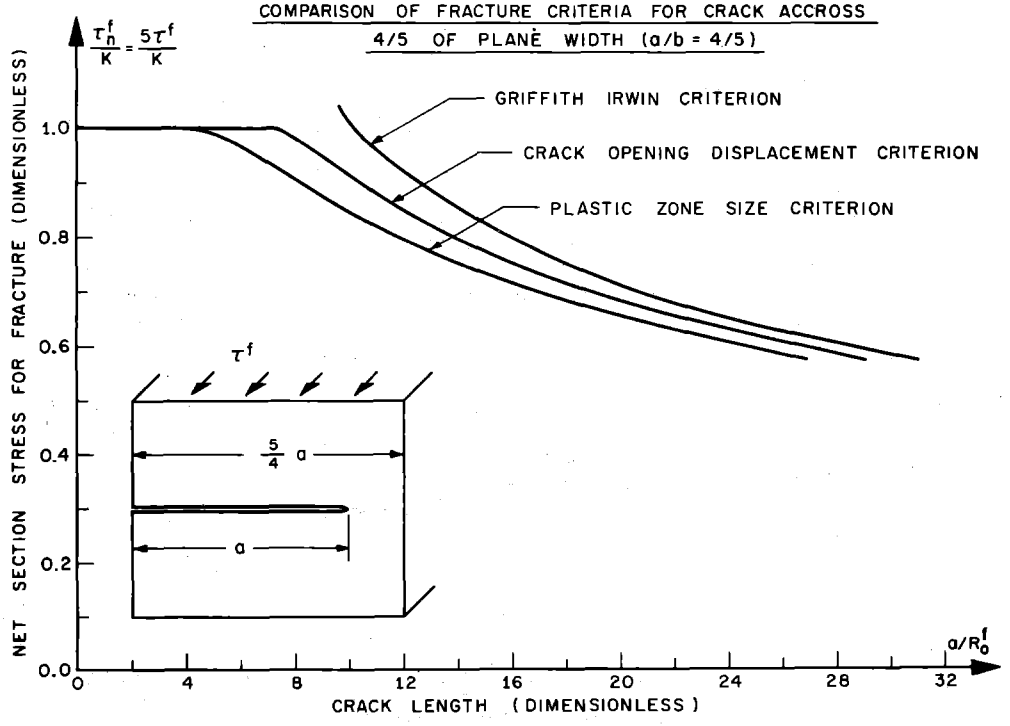
COMPARISON OF FRACTURE CRITERIA FOR CRACK ACCROSS
4/5 OF PLANE WIDTH (a/b = 4/5)
$\frac{\tau_n^f}{K} = \frac{5\tau^f}{K}$
GRIFFITH IRWIN CRITERION
CRACK OPENING DISPLACEMENT CRITERION
PLASTIC ZONE SIZE CRITERION
$\tau^f$
$\frac{5}{4}$ a
a
NET SECTION STRESS FOR FRACTURE (DIMENSIONLESS)
1.0
0.8
0.6
0.4
0.2
0.0
0
4
8
12
16
20
24
28
32
$a/R_o^f$
CRACK LENGTH (DIMENSIONLESS)

Fig. 12

plane width ratios of 0 (infinite width), 2/5, and 4/5, respectively. The criterion based on the elastic solution is seen to be at variance everywhere but at low stress levels. More alarming, however, is the fact that the two different measures of local crack tip deformation, as taken from the elastic-plastic solution, are considerably at variance with each other for all three size ratios.

This discrepancy suggests the necessity of considering the micro-structural details of material separation in deriving a satisfactory fracture criterion; the expedient method of basing fracture conditions on parameters from a continuum solution describing the local crack tip deformation is unambiguous only for fractures at low net section stresses. Methods of relating continuum solutions to micro-structural details have been discussed by Rice,[17] in an examination of a Griffith-type theory employed in conjunction with elastic-plastic continuum solutions, and by McClintock,[18] assuming fracture to be due to the growth and coalescence of voids in front of a crack. The work of [17] points out the necessity of obtaining realistic work-hardening solutions for prediction of brittle fracture strength via an energy balance approach for ductile materials.

While an unambiguous measure of fracture strength cannot be obtained solely from continuum considerations, it appears likely that the fracture criterion here presented, as based on a critical plastic zone size (or, equivalently, on strains in front of the crack line), does give a lower bound to the fracture strength of a real material. First, being based on local strains instead of on some averaging of the deformations throughout the plastic zone, it appears to be the local measure from a perfect plasticity solution most at variance with elastic predictions; further, being based on perfect plasticity, it is expected to over-estimate the severity of local deformations in actual work-hardening materials. It is therefore suggested that the elastic Griffith-Irwin criterion and the elastic-perfectly plastic critical zone size criterion provide, respectively, upper and lower bounds to the size dependence of fracture strength, in the sense that the behavior of real materials lies somewhere between the extreme criteria in Figures 10 - 12.

The elastic-plastic response to fluctuations in applied load is of interest in studies dealing with fatigue crack propagation. When the loading is of a cyclic nature with constant amplitude and fixed mean value, the complete plasticity solution is readily obtained from our results for monotonic loading. Suppose a loading $\tau$ is applied and then decreased an amount $\Delta\tau$ so that the applied stress is then $\tau - \Delta\tau$. The unloading induces reverse yielding, and so long as the zone of reversed yielding is contained within the original plastic zone, the effective yield stress is 2k. Therefore, the size and shape of the reversed yield zone is given by the formulae for monotonic loading with $\tau$ replaced by $\Delta\tau$ and k replaced by 2k. Similarly, the change in plastic strains and displacements due to unloading are given by previous expressions with the same substitutions. This simple procedure is valid since the original plastic flow is radial in the sense that the direction of the stress vector is constant at points undergoing yielding. When the applied stress is increased from $\tau - \Delta\tau$ to $\tau$, completing the cycle, the original solution is recovered.

In particular, if the body is completely unloaded ($\Delta\tau = \tau$), one may show for the case of small scale yielding that the reversed plastic zone size is one quarter of the original zone size and that the residual crack opening displacement and strains in the reversed zone are one half the original values. These results are pertinent to experimental studies of plastic deformation carried out after unloading.

Fracture under tensile loadings, rather than by longitudinal shearing, is of primary interest. Thus the results of this paper on finite width effects, as well as recently obtained solutions for the anti-plane loading of plastically anisotropic[19] and strain hardening[20,21] materials, cannot

reliably be made a basis for fracture prediction until the extent of relevance to in-plane loading situations is better established. Certainly, in seeking grounds for analogy, it is unreasonable to expect any direct correspondence in detailed features of the crack tip strain and stress distribution. Rather, analogy should be sought on the basis of gross features or integrated effects of the analysis. For example, predictions of plastic zone sizes, crack opening displacements, and in particular, resulting criteria for stable and unstable crack propagation, as well as the modifications accruing from variations of specimen geometry, yield conditions, and hardening behavior, should form the basis for attempts at comparison with tensile experimental results. McClintock and Irwin[7] have pointed out, for example, that longitudinal shear predictions of the amount of slow growth preceding fracture and plane stress size effects are in agreement with the trend of available data. The possibility of a hydrostatic buildup of stress causes ambiguity in the choice of a yield strength, to replace k of the shear analysis, under plain strain conditions. To the extent that slip-line theory[12] is appropriate for compressible elastic materials, any slip line emanating from the crack surface and crossing the line of symmetry in front of the crack swings through a $90^{\circ}$ angle, so that the effective yield strength might be taken as $(1+\pi/2)$ times the tensile strength, as in the limit solution for a smooth punch.[12] This is generally inconsistent at high stress levels, however, unless the geometry is of the double edge notch type[7] so that the hydrostatic stress build-up persists up to limit load.

## ACKNOWLEDGEMENT

This work was carried out under the financial support of a National Academy of Sciences - National Research Council postdoctoral fellowship funded by the Air Force Office of Scientific Research. This financial assistance, as well as that of the Advanced Research Projects Agency in the preparation of the manuscript, is gratefully acknowledged.

Gratitude is also expressed to Dr. George R. Irwin of the Naval Research Laboratory for suggesting consideration of the problem treated and for pointing out some simplifications of the analytical results.

Received November 1, 1965.

## REFERENCES

1. D.S.Dugdale — J. Mech. Phys. Solids, 8 (1960).
2. J.N.Goodier; F.A.Field — Fracture of Solids, eds. Drucker and Gilman, Wiley (1963).
3. J.R.Rice — "Plastic Yielding at a Crack Tip", to appear in Proc. of Intl. Conf. Fracture, Sendai, Japan (1965).
4. J.A.H.Hult; F.A.McClintock — Ninth Int. Cong. Appl. Mech., 8, Brussels (1956).
5. F.A.McClintock — ibid ref. 2.
6. M.F.Koskinen — Trans. ASME, J. Basic Engr., 85D (1963).
7. F.A.McClintock; G.R.Irwin — Proc. ASTM Symp. on Crack Toughness Testing and Applications (June 1964).
8. O.L.Bowie — J. Appl. Mech., 31, 2 (June 1964).

9. A.S.Kobayashi; R.B. Cherepy; W.C.Kinsel — J.Basic Engr., 86, 4 (Dec. 1964).

10. B.Gross; J.E.Srawley; W.F.Brown, Jr. — "Stress Intensity Factors for a Single-Edge-Notch Tension Specimen by Boundary Collocation of a Stress Function," NASA TN D-2395, Lewis Research Center (Aug. 1964).

11. G.R.Irwin — J.Appl.Mech., 24 (June 1957).

12. W.Prager; P.G.Hodge, Jr. — Theory of Perfectly Plastic Solids, Wiley (1951).

13. G.R.Irwin — Structural Mechanics, Pergamon Press (1960).

14. P.C.Paris; G.C.Sih — ibid ref.7.

15. G.R.Irwin; M.F.Koskinen — Disc.and author's closure for ref.6.

16. B.A.Bilby; A.H.Cottrell; K.H.Swinden — Proc.Roy.Soc. A, 272 (1963).

17. J.R.Rice — "An Examination of the Fracture Mechanics Energy Balance from the Point of View of Continuum Mechanics," ibid ref.3.

18. F.A.McClintock — "A Criterion for Ductile Fracture by the Growth of Holes," Mass.Inst.of Tech.Technical Report (1964).

19. J.R.Rice — "On the Theory of Perfectly Plastic Anti-Plane Straining," Brown U.Tech. Report NSF-GK-286/2 (March 1966).

20. H.Neuber — J.Appl.Mech., 28 (Dec.1961).

21. J.R.Rice — "Stresses Due to a Sharp Notch in a Work Hardening Elastic-Plastic Material Loaded by Longitudinal Shear," Brown U.Tech.Report NSF-GK-286/1 (Dec. 1965).



RÉSUMÉ - Une solution linéaire exacte, élastique - parfaitement plastique, est présentée pour le problème d'une entaille aigue (ou, quand l'angle de l'entaille est égal à zéro, und fissure), dans un plan d'étendue finie, sujette à des contraintes antiplanes qui induisent une contrainte et une déformation de cisaillement longitudinale.

Des solutions générales pour les coordonnées physiques qui correspondent aux contraintes données, la position de la limite élastique - plastique, et les déplacements qui en résultent sont données sous forme d'intégrales simples finies.

Le cas des fissures est discuté en détail et des solutions de forme fermée présentées en terme de functions élémentaires et elliptiques. Les résultats numériques sont donnés et les applications de la solution au développement d'un critère de fracture ainsi que quelques difficultés inhérentes sont discutées.



ZUSAMMENFASSUNG - Eine exakte linear elastisch-perfekt plastische Lösung wird für das Problem einer scharfen Kerbe (oder, wenn der Winkel der Kerbe null ist, für einen Anriss), in einer Ebene mit endlicher Breite gezeigt, die mit einer Längsschubspannung beansprucht wird. Allgemeine Lösungen für Koordinaten die den gegebenen Soannungen entsprechen, für den Ort der elastisch-plastischen Grenze sowie für die dazuge hörenden Verformungen werden in Form von endlichen Einfachintegralen gegebenen.

Der Fall der Risse wird im Detail behandelt. Die Lösungen sind in geschlossener Form, in elementaren und elliptischen Funktionen angegeben.

Numerische Resultate werden gegeben und die Anwendung der Lösungen zur Entwicklung der Kriterien der Bruchmechanik, sowie einige anhaftende Schwierigkeiten werden besprochen.